



Processing dates: received on 2026-1-16, reviewed on 2026-02-23,  
accepted on 2026-04-08 and online availability on 2026-04-25

## Impact of surface roughness on the adhesion strength of PVA/eggshell-derived hydroxyapatite coatings on AISI 316L substrates

Mochamad Arif Irfa'i<sup>1\*</sup>, Suherman<sup>2</sup>, Achmad Fadjar Maulana Firdaus<sup>3</sup>

<sup>1</sup>Department of Mechanical Engineering, Universitas Negeri Surabaya, Surabaya 60231, Indonesia

<sup>2</sup>Department of Mechanical Engineering, Universitas Muhammadiyah Sumatera Utara, Medan 20238, Indonesia

<sup>3</sup>Department of Material and Metallurgical Engineering, Institut Teknologi Sepuluh Nopember, Surabaya 60111, Indonesia

\*Corresponding author: arifirfai@unesa.ac.id

### Abstract

This study investigates the effect of AISI 316L surface roughness on the adhesion Poly Vinyl Alcohol (PVA) and eggshell-derived Hydroxyapatite (HA) coatings applied via slurry spraying. The surfaces were modified by the sandblasting method resulting in a maximum roughness of 4.803  $\mu\text{m}$  using 16-30 mesh  $\text{SiO}_2$  as sandblasting media. Reducing  $\text{SiO}_2$  particle size to 30-60 mesh and subsequently 60-80 mesh, gradually reduces the surface roughness to 3.431  $\mu\text{m}$  and 1.712  $\mu\text{m}$ , proving that smaller abrasive particles result in a smoother surface. The slurry spraying process was then done using 27:73 mass-based mixture of HA and 3% PVA solution in water. Results revealed that while sandblasting significantly altered substrate topography, the resulting coatings remained dense and pore-free with consistent thickness across all roughness levels, while maximum adhesive strength of 4.09 MPa based on ASTM D4541 method was observed in the specimen sandblasted with 30-60 mesh  $\text{SiO}_2$ , corresponding to a  $R_a$  value of 3.43  $\mu\text{m}$ . Utilizing sustainable eggshell-derived HA provides a bioactive, cost-effective coating material that achieves high inter facial adhesion on AISI 316L, offering a mechanically stable and affordable solution for the development of next-generation orthopedic implants.

### Keywords:

Coating, hydroxyapatite, poly vinyl alcohol, surface roughness AISI 316L, pull-off adhesion.

### 1 Introduction

Total hip replacement or Total Hip Arthroplasty (THA) is one of the most successful surgeries for treating end-stage degenerative hip osteoarthritis. Compared to other treatments available, this procedure reliably improved patients' quality of life, restoring hip functionality, and effectively reducing hip pain [1]. For this surgery, an implant, usually made from titanium alloy or cobalt-chromium alloy, is used to permanently replace the hip joint. As of today, implants made from said alloys still have a high-cost barrier, limiting THA exercise due to cost limitations [2]. By 2050, the prevalence of hip osteoarthritis in Indonesia is expected to rise by 240% for women and 310% for men compared to 1990 numbers [3]. The increasing risk of osteoarthritis and the limiting factor of implant cost urges the development of an affordable implant to be used for hip replacement.

AISI 316L stainless steel is one of the more affordable materials that is well known to be bio-compatible and durable enough inside human body environments, especially when used for a short

duration, such as fracture plate and fracture bolt [4]. However, the usage of AISI 316L in a permanent manner inside the human body is known to be disruptive to bone growth due to poor osseointegration of AISI 316L into the bone matrix. Additionally, prolonged exposure to body fluid can cause metal ion release into the surrounding tissue, potentially initiating allergic reactions [5], [6]. To address those concerns, several coating materials such as Hydroxyapatite (HA), Poly Vinyl Alcohol (PVA), TiN, etc. have been developed to shield AISI 316L from body fluid and promote better osseointegration [7], [8], [9].

HA is a crystalline mineral commonly found in the human body as a constituent of hard tissue such as bone and teeth. As it is already present inside the human body, HA has become one of the most prevalent materials to be used for implant coating due to its bioactivity and biocompatibility. The bioactive aspect of HA significantly enhances osseointegration between the implant and bone matrix while also shielding the implant from bodily fluids, blocking metal ions from dissolving into the body [7], [10]. HA itself can be produced either synthetically or derived from organic waste materials such as cattle bones, marine animal scales, or even eggshells. Compared to synthetic HA, these natural sources contain several trace ions such as  $\text{Na}^+$ ,  $\text{Mg}^{2+}$ , and  $\text{Al}^{3+}$  that substitute some  $\text{Ca}^{2+}$  positions in HA. These trace ions mimic the natural apatite composition produced by the human body, thus increasing the bone regeneration and reformation and making natural HA source more favourable [11]. Especially for eggshell-derived HA, a higher crystallinity compared to synthetic HA is observed, further improving osteogenic cell proliferation around the implants [12]. Along with the abundance of eggshell waste and considerably lower cost compared to other sources, eggshell-derived HA presents sustainable and high-quality feedstocks to be used as implant coatings.

Present technology commonly used to coat HA on metal surfaces include electrodeposition, plasma spraying, sol-gel, and PVD techniques. While each of the said methods has been successfully used to deposit HA on a metallic surface, several drawbacks still occur, such as unintentional phase change, porosity, low adhesion, and high sensitivity to coating environments [13]. Much of this unwanted effect came from the high temperature differential that is present during the coating process. However, applying HA by itself at a lower temperature results in lower HA adhesion, reducing mechanical properties and biocompatibility of the coating [10]. To apply HA at low temperatures, a combination of HA and a film-forming agent that is excellent to coat the metallic substrate in low temperatures is needed. PVA is a non-toxic synthetic polymer that has good biocompatibility and behaves as an exceptional film-former that can bond with both HA and metallic surfaces and such, have a favourable effect on increasing the mechanical properties of HA coatings on AISI 316L surface [14], [15].

While an additional binder is much needed to strengthen the bond between HA and the substrate, an optimal application method is also a key factor in achieving good coatings. Slurry spraying is one of the more preferred methods for depositing aerosolized coating materials, such as PVA/HA composites, to metal surfaces. In addition to preventing phase change in HA, slurry spraying also excels in maintaining substrate conditions, eliminating possibilities of substrate deformation or sensitization due to high temperature [16]. Fundamentally, slurry spraying works by accelerating aerosol until its kinetic energy is able to deform the aerosol particles and anchoring the particles to metal substrate upon impact due to solid-state bonding [17]. Achieving satisfactory coatings properties via slurry spray depends on several factors, which include critical spray velocity, particle density, particle shape, and particle fracture energy [18]. Study by Aminatul, *et al.* revealed that spray pressure and spray distance affect the results of PVA/HA coating, where higher pressure and further distance caused a thicker coating thickness [19].

Besides those factors, interaction between particles and substrate is largely influenced by the Coefficient of Restitution (CoR) of the surface pairs. Lower CoR results in higher energy absorbed by particles and substrate, resulting in higher deformation experienced by both surfaces. It is widely known that CoR is largely affected by surface roughness. Li, *et al.* reported that increasing surface roughness resulted in lower CoR at the same impact velocity, which consequently increased the adhesive force between the substrate and particles [20]. Additionally, increasing surface roughness provides mechanical interlocking and larger surface area for bonding, further affecting the characteristics of resulting coatings [21], [22]. Previous research has predominantly focused on the adhesion mechanisms of pure HA coatings, which often suffer from interfacial brittleness [23], [24], or synthetic polymer/HA composites like PCL/HA, where the polymer matrix serves as a rigid structural support [25]. However, the use of PVA introduces a unique viscoelastic component that may enhance energy dissipation during impact, while the biogenic origin of eggshell-derived HA offers a distinct particle morphology compared to synthetic variants. As far as we are concerned, there is no study that focuses on the effect of substrate surface roughness on PVA/HA coating characteristics. A rougher surface can provide a larger surface area and more anchor points for the coating slurry attachments. However, a surface too rough can also cause sharp discontinuities in coating thickness, potentially causing cracks and uneven coatings, especially for coating systems that use liquid phase as the carrier [26], [27]. Therefore, this study presented a novel experimental approach to understanding the effect of surface roughness on the thickness and adhesion strength of PVA/HA coatings on AISI 316L stainless steel.

## 2 Materials and methods

### 2.1 Materials

HA powder is extracted from chicken eggshell obtained as organic waste from a traditional market in Surabaya, Indonesia according to methods developed by previous studies [11], [28]. Fully hydrolyzed PVA bead (P1763) with  $M_w$  of 89,000–98,000 g/mol and ethanol (96% w/v) was obtained from Sigma-Aldrich, USA. AISI 316L stainless steel (Initial  $R_A$ : 0.5  $\mu\text{m}$ ) and silica sand are obtained from local suppliers in Surabaya, Indonesia.

### 2.2 AISI 316L surface preparation

Surface preparation of AISI 316L substrate is done according to the ISO 8501-1 standard. Firstly, solvent cleaning is used to remove grease, oil, and dirt from metal surfaces. Subsequently, the abrasive blasting process is done using a pressure of 0.7 MPa, a blasting angle perpendicular to substrate, a blasting time of 15 seconds, and a blasting distance of 150 mm. An AISI 316L plate with a 50 mm×50 mm×3 mm dimensions is used as metal substrate for the experiment. The blasting media used is silica sand ( $\text{SiO}_2$ ) with varied particle size (coarse: 16–30 mesh, medium: 30–60 mesh, and fine: 60–80 mesh). Final surface roughness value obtained after the surface preparation process is verified by Mitutoyo SurfTest SJ-310 Roughness Meter calibrated to the ASTM D4411 standard with triplicate measurements.

### 2.3 PVA/HA solution preparation

The PVA solution is prepared by dissolving 3 g of PVA beads in 70 g deionized water, followed by stirring using a magnetic stirrer at 250 rpm until all the PVA beads are dispersed and heating to 80°C until a solution is formed. The process is then finished by cooling the mixture to a temperature of 65°C to avoid a drastic increase of the mixture's viscosity at a lower temperature. The heating steps ensure quick and homogenous dissolution of PVA in deionized water and prevent aggregations of PVA slurry. Afterwards 27 g of HA powder is added to the mixture followed by stirring for 180 minutes. Finally, the PVA/HA solution is left overnight before use.

## 2.4 PVA/HA coating on AISI 316L substrate

The PVA/HA coating process is done by slurry spray methods with spraying parameters described in Table 1.

Table 1. PVA/HA coating parameters

Parameters	Value
Pressure	700 kPa
Nozzle distance	150 mm
Nozzle shape/size	Cylindrical, $\varnothing$ 0.5 mm
Flow regime	Subsonic
Feed rate	Unrestricted slurry flow based on venturi effect
Spraying angle	90°
Spraying direction	Unidirectional
Layer counts	6
Pass per layer	1
Interpass time	60 seconds
Single spray duration	2 seconds
Relative humidity	<85%
Substrate temperature	Dew point + 3°C

After the PVA/HA layer is successfully coated on an AISI 316L stainless steel surface, the drying process is done by heating the coated plate inside the Nabertherm drying furnace at a temperature of 80°C for 24 hours. The coating process is triplicated for each surface roughness variation to ensure the repeatability of the process.

## 2.5 Characterizations

The coated substrate is characterized by its coating thickness, adhesive strength, and surface microstructure. Adhesive strength of the PVA/HA coating is measured in triplicate using Positest ATM20 portable adhesive strength tester equipped with an aluminum dolly conforming to ASTM D4541 standards. Surface morphology's characterization was done using a Hitachi TM3000 Scanning Electron Microscope (SEM) with a BSE detector. The resulting image is then processed to obtain the coating thickness in various SS316L surface roughness.

## 3 Results and discussion

### 3.1 Surface roughness of SS316L after surface preparation

Surface preparation using sandblasting was done with a variation in sand particle size. Visually, the appearance of the plate changed from shiny luster in as-rolled SS316L into a dull appearance after the sandblasting process. Additionally, many small craters with various depths and diameters were observed. Bigger craters were observed in the plate subjected to coarser sand particles. The visual appearance of SS316L before and after the sandblasting process is documented in Fig. 1.

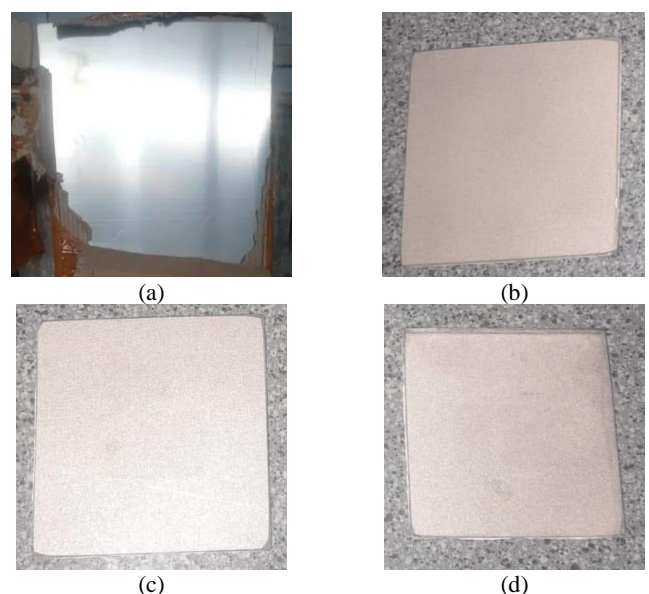


Fig. 1 (a) SS316L plate before sandblasting and after sandblasting with (b) 60–80 mesh particle, (c) 30–60 mesh particle, and (d) 16–30 mesh particle.

The reduction in shiny luster of the plate was caused by light scattering due to increasing roughness of the surface after shooting with sand particles [29]. The average roughness ( $R_a$ ) value of the SS316L plate was measured quantitatively, and the results described in Fig. 2.

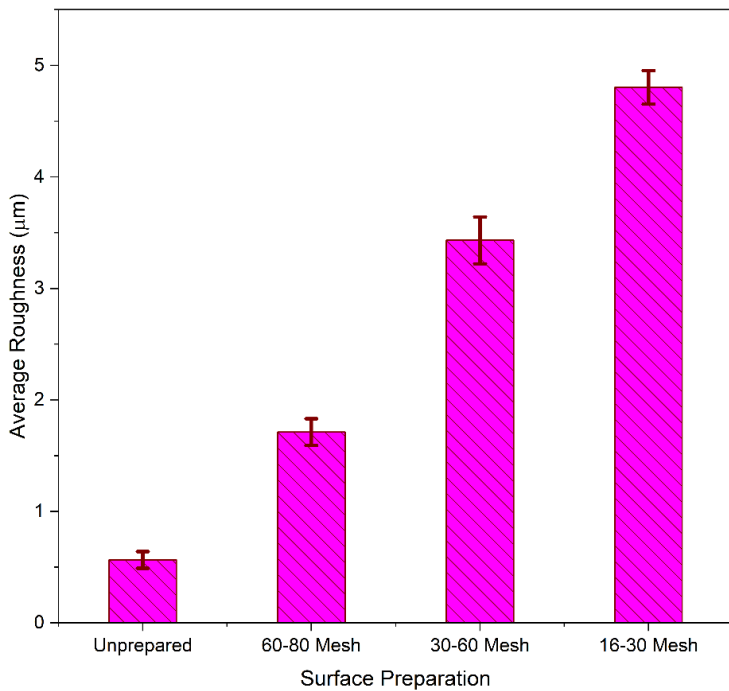


Fig. 2.  $R_a$  value of SS316L plate with various surface preparation.

The resulting surface roughness is seen increasing alongside the increase of abrasive particle. The unprepared surface has the lowest roughness value, amounting to  $0.565 \mu\text{m}$ . The sample abraded with the highest particle size (16-30 mesh) exhibited the highest surface roughness value of  $4.803 \mu\text{m}$ . Other samples have an average roughness value in between those two samples. The SS316L plate treated with 60-80 mesh abrasive has  $1.712 \mu\text{m}$  roughness, while the sample treated with 30-60 mesh sand have a roughness of  $3.431 \mu\text{m}$ . The results aligned with the visual appearance of the plate in Fig. 1, where the unprepared plate has the shiniest appearance, and the plate sandblasted with coarse sand particles has a matte appearance.

### 3.2 Morphology and HA/PVA coating thickness on sandblasted SS316L plate

The cross-sectional morphology of SS316L coated with HA/PVA can be observed in Fig. 3. All three samples showed a dense coating with no pores observed in the SEM image. These findings showed that the wettability of the sandblasted SS316L plate is good and the HA/PVA slurry can spread out evenly on its surface. On the plate sandblasted with finer abrasives, the interface between metals and coatings formed a nearly straight line, proving that finer abrasives do not leave a huge dent in the steel. A sample sandblasted with a medium-sized abrasive showed several microcracks under the surface that was not filled with HA/PVA coating. These phenomena showed that a medium-sized abrasive caused a small but relatively deep dent which is able to initiate microcracks in the subsurface of the plate. As for the interface between stainless steel and the coating, several gentle valley and hill pattern patterns were observed, indicating that the bigger abrasive particle is succeeded in deforming the plate surface.

The plate sandblasted with the coarse abrasive showed a very rough interface between the coating and the stainless steel. However, no microcrack is observed in this variation. The absence of microcrack in this variation is the result of the bigger kinetic energy of the coarser and heavier abrasive that can chip away the metal directly as seen in the rough surface developed. As the energy is enough to chip the surface, any microcrack developing on

the surface during sandblasting is converted into a total fracture and knocks small pieces of the plates off [30].

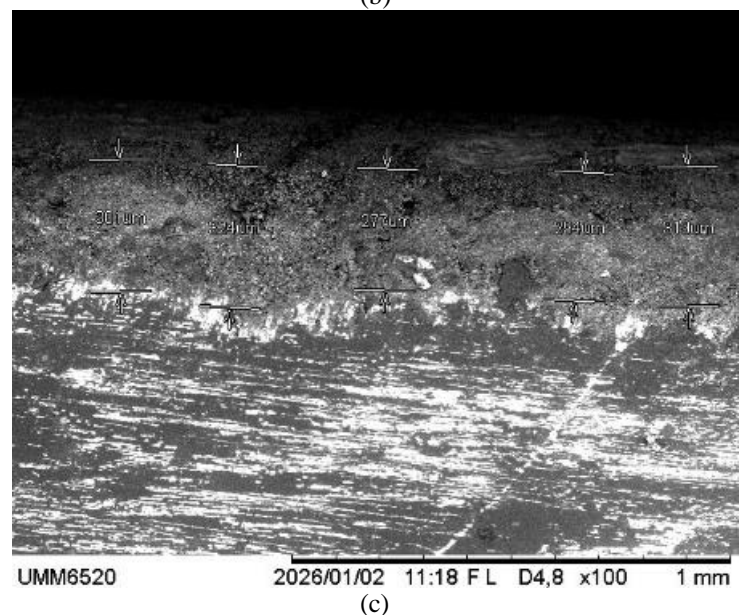
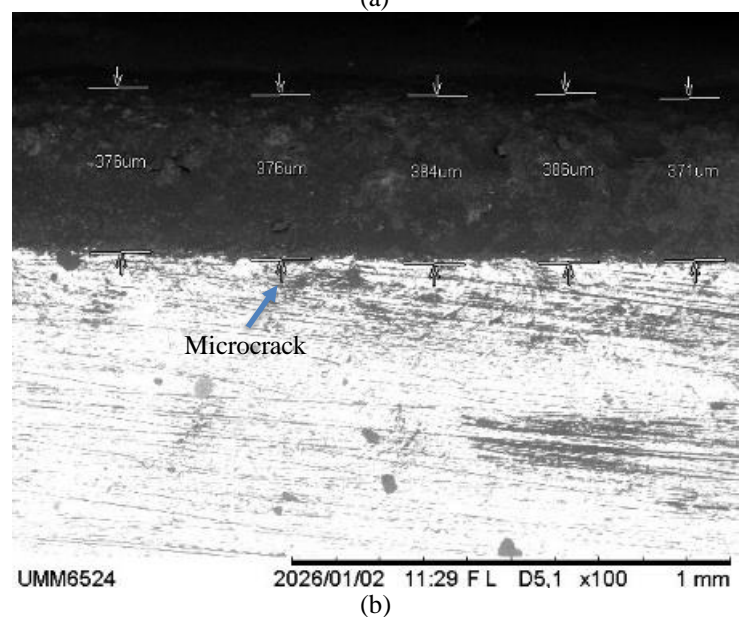
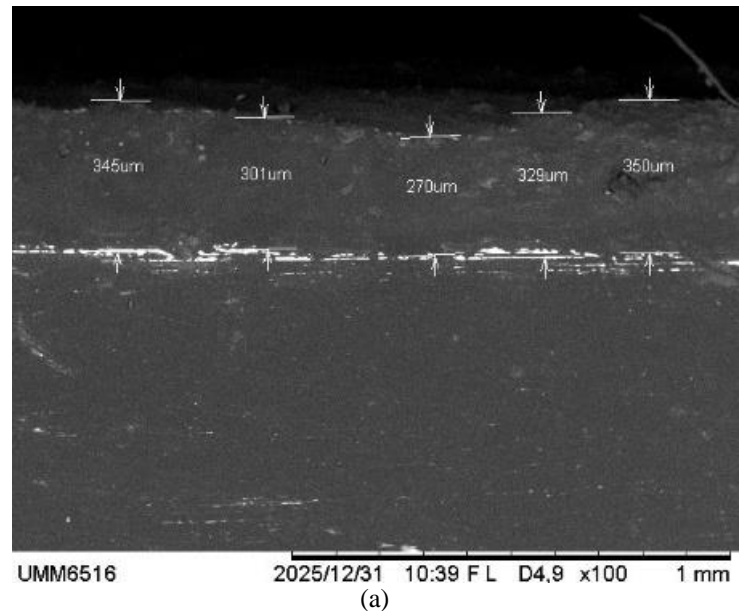


Fig. 3. Cross-section SEM image of HA/PVA coated on SS316L sandblasted with (a) 60-80 mesh abrasive, (b) 30-60 mesh abrasive, and (c) 16-30 mesh abrasive, 100 $\times$  magnification.

The resulting coating thickness obtained in all specimens does not vary significantly with changing roughness of the substrate. Coating at plate sandblasted with finer abrasives has  $321 \pm 35.9 \mu\text{m}$

thickness, the plate sandblasted with medium-sized abrasives have  $378.6 \pm 6.22 \mu\text{m}$  coating thickness, and the plate sandblasted with coarse abrasive have  $299.8 \pm 19.6 \mu\text{m}$  coating thickness. The coating thickness was largely similar to other slurry-sprayed systems. Ohtsu, *et al.* reported a thickness of around  $300 \mu\text{m}$  on a Hydroxyapatite –  $\text{TiO}_2$  slurry-based coating system [31]. However, Fadli, *et al.* managed to influence the coating thickness by varying the hydroxyapatite concentration inside the slurry, successfully increased the coating thickness from  $125 \mu\text{m}$  to  $225 \mu\text{m}$  by increasing the HA concentration in the slurry from 31% wt to 42% wt [32]. As this research does not vary the slurry compositions, it is inferred that the coating thickness remains the same for the variations.

The identical coating thickness and the absence of porosity showed that substrate roughness does not affect the soundness and structural integrity of PVA/HA coatings.

### 3.3 Adhesive strength of HA/PVA coating on sandblasted SS316L plate

The ASTM D4541 method (pull-off) test is used for assessing the adhesive strength of HA/PVA coating and the resulting data is displayed in Fig. 4. As can be deduced from the SEM image in Fig. 3, the specimen with the smallest cross-section, which is

sandblasted using the fine (60-80 mesh) abrasive, has the lowest adhesive strength of the three specimens with a value of  $3.46 \pm 0.75 \text{ MPa}$ . The low adhesive strength of this variation is caused by the small interface between substrate and coating observed in the specimen. The straight line interface particularly has very low mechanical interlocking between the substrate and the coating, allowing the coating to easily slip and detach from the substrate [33].

Specimens sandblasted with a medium-sized abrasive (30-60 mesh) surprisingly had the highest adhesion strength of all specimens tested with a value of  $4.09 \pm 0.30 \text{ MPa}$ . The high adhesive strength of this specimen is caused by the addition of shallow creases and valley caused by plastic deformation upon impact with the abrasive. The smooth but uneven surface of the SS316L substrate increased the interface area between the substrate and coating, thus increasing its adhesive strength. Increasing the abrasive size in the sandblasting process does not cause further increase in adhesive strength. The specimen sandblasted with 16-30 mesh abrasive has  $3.90 \pm 0.38 \text{ MPa}$  adhesive strength. The slight decrease in adhesion strength is caused by a decrease in penetration ability of HA/PVA slurry to fill the deep and sharp gap observed in the substrate [34].

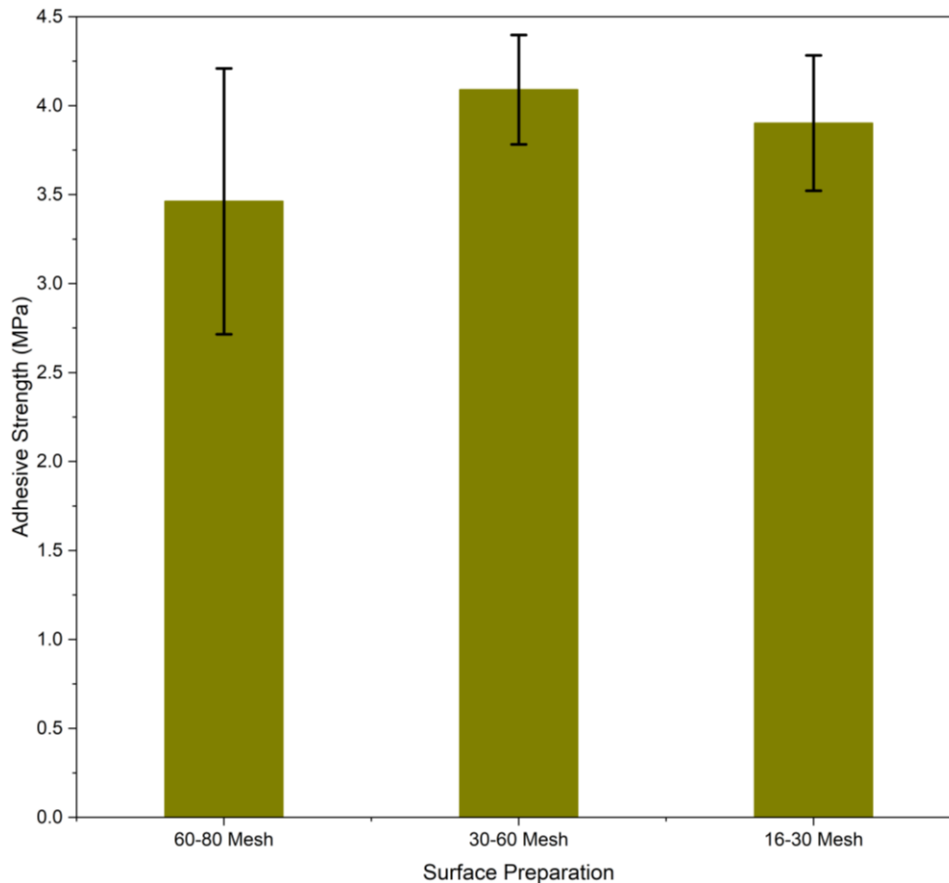


Fig. 4. Adhesive strength of HA/PVA coating on sandblasted SS316L.

Adhesion failure of HA/PVA coating on SS316L can be defined as a combination of adhesive and cohesive failure, where the adhesive failure occurs at the interface between substrate and coating while cohesive failure occurs between successive layers of coatings [35], [36]. The failure mode of HA/PVA coating is shown in Fig. 5.

The specimen sandblasted with a fine abrasive showed dominant adhesive failure as more substrate is exposed after failure, while the specimen with the best adhesive strength, which is the specimen sandblasted with a medium-sized abrasive, has much less adhesive failure. The specimen that was sandblasted using a coarse abrasive exhibited a balanced failure mode, with roughly half the failure face being cohesive, and another half in adhesive failure mode.

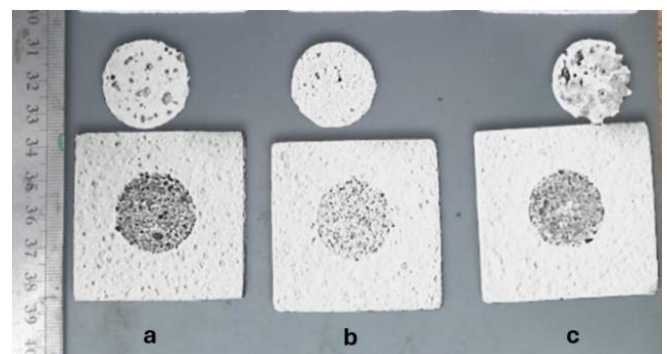


Fig. 5. Failure face of HA/PVA coating on SS316L sandblasted with with (a) 60-80 mesh abrasive, (b) 30-60 mesh abrasive, and (c) 16-30 mesh abrasive.

## 4 Conclusions

This research demonstrates that sandblasting effectively modifies the AISI 316L surface, with coarser abrasive particles significantly increasing average roughness from 0.565  $\mu\text{m}$  to 4.803  $\mu\text{m}$ . A consistent trend was observed, where smaller abrasive sizes produced lower roughness values of 3.431  $\mu\text{m}$  and 1.712  $\mu\text{m}$  for 30–60 mesh and 60–80 mesh particles, respectively. The slurry spray deposition of the PVA/eggshell-derived HA composite produced a dense, pore-free coating, indicating excellent wettability and adhesion on the sandblasted steel. SEM observations revealed that coarse-grit blasting produced a rougher interface and localized sub-surface microcracks; however, the coating thickness remained uniform across different surface conditions. These results indicate that mechanical interlocking induced by sandblasting enhances interfacial bonding without significantly altering coating structure. Silica particle in the range of 30–60 mesh was found to be the most optimal abrasive for PVA/HA coating preparations as it resulted in superior adhesive strength of  $4.09 \pm 0.30$  MPa. Ultimately, the use of sustainable eggshell-derived HA and a PVA binder provides a bioactive and commercially affordable alternative to high-cost alloys. This approach proves that optimal surface preparation is critical for good coating adhesion and provides a valuable starting point in the development of hip replacements replacement implants in cost-sensitive healthcare environments by improving biocompatibility and structural integrity of the implant while reducing implant cost. Further studies shall be directed in finding the correlation of abrasive particle shape and hardness to the formation of microcracks in the substrate in order to create the most optimal surface profile for the adhesion of HA/PVA coatings.

## References

- [1] M. A. Varacallo, T. D. Luo, and N. A. Johanson, *Total Hip Arthroplasty Techniques*. Treasure Island, Florida: StatPearls Publishing LLC., 2025.
- [2] C. C. Barber, M. Burnham, O. Ojameruaye, and M. D. McKee, “A systematic review of the use of titanium versus stainless steel implants for fracture fixation,” *OTA Int.*, vol. 4, no. 3, p. e138, Sep. 2021, doi: 10.1097/OI9.000000000000138.
- [3] A. K. Gan, S. Rahman, A. Indra Nur Alam, and B. Paterasari, “Profile of Patients’ Osteoarthritis at Tertiary and Teaching in Aceh, Indonesia,” *Surabaya Physical Medicine and Rehabilitation Journal*, vol. 5, no. 1, pp. 25–31, Feb. 2023, doi: 10.20473/spmrj.v5i1.36881.
- [4] JB. Marcomini, C. A. R. P. Baptista, J. P. Pascon, R. L. Teixeira, and F. P. Reis, “Investigation of a fatigue failure in a stainless steel femoral plate,” *J. Mech. Behav. Biomed. Mater.*, vol. 38, pp. 52–58, Oct. 2014, doi: 10.1016/j.jmbbm.2014.06.011.
- [5] K.-K. Chew, S. H. S. Zein, and A. L. Ahmad, “The corrosion scenario in human body: Stainless steel 316L orthopaedic implants,” *Nat. Sci. (Irvine)*, vol. 04, no. 03, pp. 184–188, 2012, doi: 10.4236/ns.2012.43027.
- [6] Y. K. Erdogan and B. Ercan, “Anodized Nanostructured 316L Stainless Steel Enhances Osteoblast Functions and Exhibits Anti-Fouling Properties,” *ACS Biomater. Sci. Eng.*, vol. 9, no. 2, pp. 693–704, Feb. 2023, doi: 10.1021/acsbomaterials.2c01072.
- [7] J. Botterill and H. Khatkar, “The role of hydroxyapatite coating in joint replacement surgery – Key considerations,” *J. Clin. Orthop. Trauma*, vol. 29, p. 101874, Jun. 2022, doi: 10.1016/j.jcot.2022.101874.
- [8] A. Samanta *et al.*, “Bio-tribological response of duplex surface engineered SS316L for hip-implant application,” *Appl. Surf. Sci.*, vol. 507, p. 145009, Mar. 2020, doi: 10.1016/j.apsusc.2019.145009.
- [9] Z. Lei, H. Liang, W. Sun, Y. Chen, Z. Huang, and B. Yu, “A biodegradable PVA coating constructed on the surface of the implant for preventing bacterial colonization and biofilm formation,” *J. Orthop. Surg. Res.*, vol. 19, no. 1, p. 175, Mar. 2024, doi: 10.1186/s13018-024-04662-7.
- [10] M. Rafiei, H. Eivaz Mohammadloo, M. Khorasani, F. Kargaran, and H. A. Khonakdar, “Hydroxyapatite-based coatings on Mg and Ti-based implants: A detailed examination of various coating methodologies,” *Heliyon*, vol. 11, no. 2, p. e41813, Jan. 2025, doi: 10.1016/j.heliyon.2025.e41813.
- [11] N. A. S. Mohd Pu’ad, P. Koshy, H. Z. Abdullah, M. I. Idris, and T. C. Lee, “Syntheses of hydroxyapatite from natural sources,” *Heliyon*, vol. 5, no. 5, p. e01588, May 2019, doi: 10.1016/j.heliyon.2019.e01588.
- [12] J. S. Swarup, R. Thomas, J. Rucharitha, V. R. Arunkumar, and V. V., “Eggshell-derived hydroxyapatite as a biomaterial in dentistry: a scoping review of synthesis, properties and applications,” *Evid. Based. Dent.*, May 2025, doi: 10.1038/s41432-025-01146-3.
- [13] D. Arcos and M. Vallet-Regí, “Substituted hydroxyapatite coatings of bone implants,” *J. Mater. Chem. B*, vol. 8, no. 9, pp. 1781–1800, 2020, doi: 10.1039/C9TB02710F.
- [14] E. Vafa, R. Bazargan-Lari, and M. E. Bahrololoom, “Electrophoretic deposition of polyvinyl alcohol/natural chitosan/bioactive glass composite coatings on 316L stainless steel for biomedical application,” *Prog. Org. Coat.*, vol. 151, p. 106059, Feb. 2021, doi: 10.1016/j.porgcoat.2020.106059.
- [15] M. I. Baker, S. P. Walsh, Z. Schwartz, and B. D. Boyan, “A review of polyvinyl alcohol and its uses in cartilage and orthopedic applications,” *J. Biomed. Mater. Res. B Appl. Biomater.*, vol. 100B, no. 5, pp. 1451–1457, Jul. 2012, doi: 10.1002/jbm.b.32694.
- [16] T.-Y. Liao *et al.*, “Multifunctional cold spray coatings for biological and biomedical applications: A review,” *Prog. Surf. Sci.*, vol. 97, no. 2, p. 100654, May 2022, doi: 10.1016/j.progsurf.2022.100654.
- [17] A. Viscusi, A. Astarita, R. Della Gatta, and F. Rubino, “A perspective review on the bonding mechanisms in cold gas dynamic spray,” *Surface Engineering*, vol. 35, no. 9, pp. 743–771, Sep. 2019, doi: 10.1080/02670844.2018.1551768.
- [18] B. Daneshian, F. Gaertner, H. Assadi, D. Hoeche, W. Weber, and T. Klassen, “Size Effects of Brittle Particles in Aerosol Deposition—Molecular Dynamics Simulation,” *Journal of Thermal Spray Technology*, vol. 30, no. 3, pp. 503–522, Feb. 2021, doi: 10.1007/s11666-020-01149-9.
- [19] Aminatun, F. F. S. B. Tenong, and D. Hikmawati, “Characterization of SS316L metal coated Hydroxyapatite-Poly vinyl alcohol through airbrush spraying method,” 2020, p. 050009. doi: 10.1063/5.0034691.
- [20] X. Li, M. Dong, D. Jiang, S. Li, and Y. Shang, “The effect of surface roughness on normal restitution coefficient, adhesion force and friction coefficient of the particle-wall collision,” *Powder Technol.*, vol. 362, pp. 17–25, Feb. 2020, doi: 10.1016/j.powtec.2019.11.120.
- [21] P. Richer, B. Jodoin, L. Ajdelsztajn, and E. J. Lavernia, “Substrate Roughness and Thickness Effects on Cold Spray Nanocrystalline Al-Mg Coatings,” *Journal of Thermal Spray Technology*, vol. 15, no. 2, pp. 246–254, Jun. 2006, doi: 10.1361/105996306X108174.
- [22] S. Kumar, G. Bae, and C. Lee, “Deposition characteristics of copper particles on roughened substrates through kinetic spraying,” *Appl. Surf. Sci.*, vol. 255, no. 6, pp. 3472–3479, Jan. 2009, doi: 10.1016/j.apsusc.2008.10.060.
- [23] C. H. Sheng, M. Nagentrau, and N. H. Ibrahim, “Prediction of brittle fracture propagation behaviour of hydroxyapatite (HAp) coating in artificial femoral stem component,” *Archives of Materials Science and Engineering*, vol. 114, no. 1, pp. 34–41, Mar. 2022, doi: 10.5604/01.3001.0015.9851.

- [24] A. Jaafar, C. Hecker, P. Árki, and Y. Joseph, "Sol-Gel Derived Hydroxyapatite Coatings for Titanium Implants: A Review," *Bioengineering*, vol. 7, no. 4, p. 127, Oct. 2020, doi: 10.3390/bioengineering7040127.
- [25] A. Prabowo *et al.*, "ADHESIVE BEHAVIOR OF POLYCAPROLACTONE/HYDROXYAPATITE COATINGS ON 316L STAINLESS STEEL: A DESIGN OF EXPERIMENTS APPROACH," *Jurnal Crystal: Publikasi Penelitian Kimia dan Terapannya*, vol. 7, no. 2, pp. 209–220, Sep. 2025, doi: 10.36526/jc.v7i2.6212.
- [26] F. Adviana, S. Ula, and Sunardi, "Study of Contact Surface Roughness on Adhesive Performance in Steel and Aluminium Joints," *DINAMIS*, vol. 12, no. 2, pp. 97–103, Dec. 2024, doi: 10.32734/dinamis.v12i2.18847.
- [27] J. P. B. van Dam, S. T. Abrahams, A. Yilmaz, Y. Gonzalez-Garcia, H. Terry, and J. M. C. Mol, "Effect of surface roughness and chemistry on the adhesion and durability of a steel-epoxy adhesive interface," *Int. J. Adhes. Adhes.*, vol. 96, p. 102450, Jan. 2020, doi: 10.1016/j.ijadhadh.2019.102450.
- [28] M. Amin, R. Ismail, J. Jamari, and A. P. Bayuseno, "Use of hydroxyapatite powder derived from green mussel shell wastes for coating on AISI 316L," *IOP Conf. Ser. Earth Environ. Sci.*, vol. 1268, no. 1, p. 012035, Dec. 2023, doi: 10.1088/1755-1315/1268/1/012035.
- [29] "Light reflection from a rough surface," in *Specular Gloss*, Elsevier, 2008, pp. 53–77. doi: 10.1016/B978-008045314-9.50007-4.
- [30] R. K. Chintapalli, A. Mestra Rodriguez, F. Garcia Marro, and M. Anglada, "Effect of sandblasting and residual stress on strength of zirconia for restorative dentistry applications," *J. Mech. Behav. Biomed. Mater.*, vol. 29, pp. 126–137, Jan. 2014, doi: 10.1016/j.jmbbm.2013.09.004.
- [31] N. Ohtsu, Y. Nakamura, and S. Semboshi, "Thin hydroxyapatite coating on titanium fabricated by chemical coating process using calcium phosphate slurry," *Surf. Coat. Technol.*, vol. 206, no. 8–9, pp. 2616–2621, Jan. 2012, doi: 10.1016/j.surfcoat.2011.11.022.
- [32] A. Fadli, "EMPIRICAL MODEL TO PREDICT THE HYDROXYAPATITE THICKNESS ON THE SURFACE OF 316L STAINLESS STEEL BY THE DIP COATING METHOD," *Ceramics - Silikat*, pp. 386–394, Nov. 2021, doi: 10.13168/cs.2021.0041.
- [33] S. J. Caraguay, T. S. Pereira, A. Cunha, M. Pereira, and F. A. Xavier, "The effect of laser surface textures on the adhesion strength and corrosion protection of organic coatings - Experimental assessment using the pull-off test and the shaft load blister test," *Prog. Org. Coat.*, vol. 180, p. 107558, Jul. 2023, doi: 10.1016/j.porgcoat.2023.107558.
- [34] S. G. Prolongo, G. Rosario, and A. Ureña, "Study of the effect of substrate roughness on adhesive joints by SEM image analysis," *J. Adhes. Sci. Technol.*, vol. 20, no. 5, pp. 457–470, Jan. 2006, doi: 10.1163/156856106777144345.
- [35] D. Bernoulli, K. Häfliger, K. Thorwarth, G. Thorwarth, R. Hauert, and R. Spolenak, "Cohesive and adhesive failure of hard and brittle films on ductile metallic substrates: A film thickness size effect analysis of the model system hydrogenated diamond-like carbon (a-C:H) on Ti substrates," *Acta Mater.*, vol. 83, pp. 29–36, Jan. 2015, doi: 10.1016/j.actamat.2014.09.044.
- [36] H. Wei *et al.*, "Adhesion and cohesion of epoxy-based industrial composite coatings," *Compos. B Eng.*, vol. 193, p. 108035, Jul. 2020, doi: 10.1016/j.compositesb.2020.108035.